THE JOURNAL OF COMPARATIVE NEUROLOGY 426:117–129 (2000)

Projections From the Medial Geniculate Body to Primary Auditory Cortex in Neonatally Deafened Cats

SUSAN G. STANTON[1–3] AND ROBERT V. HARRISON[1,2,4]*
[1]Auditory Science Laboratory, Otolaryngology/Brain and Behavior, The Hospital for Sick Children, Toronto, Ontario M5G 1X8, Canada
[2]Department of Physiology, University of Toronto, Toronto, Ontario M5S 1A1, Canada
[3]Department of Communication Sciences and Disorders, University of Cincinnati, Cincinnati, Ohio 45267-0394
[4]Department Otolaryngology University of Toronto, Toronto, Ontario M5S 1A1, Canada

ABSTRACT

In the present study, anatomical projections from the medial geniculate body (MGB) to primary auditory cortex (AI) were investigated in normal adult cats and in animals that were neonatally deafened with the ototoxic drug amikacin. Cochleotopic/tonotopic maps in AI (based on neural response characteristic frequency) were obtained with microelectrode recording techniques, and single or multiple injections of retrograde tracers (horseradish peroxidase and fluorescent dyes) were introduced into AI. The AI maps of the amikacin-treated cats had an abnormal cochleotopic organization, such that deprived cortical areas exhibited an expanded representation of intact regions of the damaged cochlea. However, retrograde tracer injections into different regions of AI produced a normal pattern of labeling in the ventral division of the medial geniculate body (MGBv). In both experimental and control animals, the main mass of labeled thalamic cells was found in the MGBv. Different isofrequency contours in AI receive input from different portions of the MGBv. Thus, cell arrays labeled by anterior AI injections were situated medially in MGBv, and injections into posterior AI labeled MGBv more laterally. Furthermore, the deafened cats did not develop a more divergent thalamocortical projection compared with normal control animals, indicating that an abnormal spread of the thalamocortical afferents across the frequency domain in AI (anterior-posterior axis) is not responsible for the altered cochleotopic map in these neonatally deafened animals. The relatively normal thalamocortical projection pattern suggests that, after neonatal cochlear lesions, the major reorganization of cochleotopic maps occurs at subthalamic levels. J. Comp. Neurol. 426:117–129, 2000.

Indexing terms: auditory system; thalamus; tonotopic; developmental plasticity; sensorineural hearing loss; cochlear lesion

In primary auditory cortex (AI) of the cat, the cochlea is represented by a functional map of sound frequency that reflects the frequency-to-place coding within the cochlea. This orderly topographic mapping of sound frequency also exists within the thalamocortical projection from the medial geniculate body (MGB) to AI. A number of studies have demonstrated that central maps representing the sensory epithelium are significantly modified by the reduced sensory input resulting from peripheral deafferentation, particularly when this deprivation occurs during early stages of development (Wiesel and Hubel, 1963a,b; Waite and Taylor, 1978).

Neuroplasticity studies in the developing auditory system have examined the effects of restricted cochlear lesions on the cochleotopic organization of the central auditory system. In AI, the representation of sound frequency develops abnormally as a consequence of long-term neonatal cochlear hearing loss (Harrison et al., 1991, 1992, 1993a,b). Areas of the tonotopic map that would normally receive input from the damaged region of the cochlea

Grant sponsor: Medical Research Council of Canada; Grant number: MA9330; Grant sponsor: The Masonic Foundation of Ontario.

*Correspondence to: Dr. Robert V. Harrison, Department of Otolaryngology, The Hospital for Sick Children, 555 University Avenue, Toronto, Ontario M5G 1X8, Canada. E-mail: rvh@sickkids.on.ca

Received 30 May 1998; Revised 23 June 2000; Accepted 23 June 2000

appear to represent the intact region near to the border of the cochlear lesion. Although these changes are observed at the cortical level, it is not clear whether they are restricted to auditory cortex or what mechanisms mediate this plasticity.

Because the thalamocortical projection may be the primary locus for changes underlying map reorganization in AI (Schwaber et al., 1993), our experiments investigated whether neonatally deafened animals with abnormal AI maps also develop a correspondingly abnormal thalamocortical projection. Mechanisms that have been suggested for the reorganization of cochleotopic representation occurring over a restricted distance in the adult AI include the unmasking, strengthening, or proliferation of synapses within the normal divergence and overlap of afferent input (Robertson and Irvine, 1989; Schwaber et al., 1993). On the other hand, functional changes that occur during the development of the auditory system appear to be more extensive and may involve structural changes, including a proliferation of local circuitry and/or of inputs from lower relay stations (Nordeen et al., 1983; Moore and Kitzes, 1985; Harrison et al., 1991, 1996). It is possible that subcortical auditory pathways associated with the deafferented portion of the cochlea may be particularly susceptible to structural modifications during the neonatal period.

Developmental studies in other sensory systems have shown that morphological changes do occur as a consequence of partial deafferentation and that abnormal patterns of sensory input during a critical postnatal period can disrupt the establishment of normal topographic order within central pathways (see, e.g., Shatz and Stryker, 1978; Pidoux et al., 1979, 1980; LeVay et al., 1980; Swindale, 1981; Jeffrey, 1984a,b; Stryker and Harris, 1986; Trevelyan and Thompson, 1992). In newborn kittens, the cochlea and the central auditory system are underdeveloped both structurally and functionally. However, during the first few postnatal weeks, after the onset of cochlear function, these structures continue to mature and may be especially influenced by abnormal patterns of sensory input (Carlier et al., 1979; Ehret and Romand, 1981; Brugge, 1983, 1988; Kitzes, 1984; Ehret, 1985; Moore, 1985; Harrison et al., 1991, 1996, 1998). Cochlear destruction in neonatal rodents leads to substantial structural and functional abnormalities in the auditory brainstem, including neural degeneration in the deafferented cochlear nucleus and altered projections from this nucleus to the inferior colliculus (Trune, 1982; Nordeen et al., 1983; Kitzes, 1984; Kitzes and Semple, 1985; Moore and Kitzes, 1985). The effects of partial cochlear lesions on the cochleotopic organization of central auditory projections has been studied in developmental models of auditory deprivation (see, e.g., Harrison et al., 1991, 1996, 1998), and the aim of the present investigation was to examine the topography of thalamocortical projections associated with reorganized cochleotopic maps in AI after long-term auditory deprivation. Thus, partial cochlear lesions were induced in neonatal kittens, and the effects of this on the development of cortical cochleotopic maps and thalamocortical connections were studied with a combination of electrophysiological and retrograde tracer techniques. We have found that, despite significant functional changes in the AI frequency map, a normal pattern of connections from MGB to AI is maintained.

MATERIALS AND METHODS

In overview, the experimental protocol was as follows: Four newborn kittens were treated with the ototoxic antibiotic amikacin to induce partial (basal) cochlear lesions bilaterally. After maturation (1.0–1.5 years of age), retrograde tracers were implanted into AI, and the frequency representation within AI was mapped using standard microelectrode recording techniques. Auditory brainstem responses (ABRs) were used to examine the extent of the cochlear lesion. Five adult cats with no detectable middle or inner ear pathology served as controls. All experiments were carried out within the guidelines set out by the Canadian Council for Animal Care and were approved by the local animal care committee at the University of Toronto.

Production and monitoring of cochlear lesions

Restricted cochlear lesions were produced by a series of daily subcutaneous injections of the ototoxic antibiotic amikacin (400 mg/kg per day) beginning on day 2 postpartum and continuing for 4 days. ABRs were used to monitor the ototoxic effects of amikacin. Skin needle electrodes in a mastoid-vertex configuration were used. Signals from the recording electrodes were amplified (×10,000) and band-pass filtered (from 150 Hz to 3 kHz). The electrical activity was sampled over a poststimulus time interval of 20 msec, and 300 sweep averages were performed (Cambridge Electronic Design 1401; hosted by a 80286 microcomputer).

ABRs were elicited using tone-burst stimuli (rise/fall time, 2 msec; 2-msec plateau; presented at a rate of 10 per second) delivered through a free-field system and calibrated at the level of the external ear canal. At each stimulus frequency used (0.5, 1, 2, 4, 8, 16, and 24 kHz), a decreasing stimulus intensity series was used to determine ABR threshold. In Figures 2 and 4–6, ABR results for the amikacin-treated cats are presented in an audiogram format, with thresholds at different stimulus frequencies plotted as a threshold shift relative to 0 dB (no hearing loss) based on the mean threshold of 11 normal hearing adult cats.

Cortical mapping

Mapping experiments were conducted on the experimental group with amikacin-induced cochlear lesions and on an untreated control group. All animals were initially anaesthetized with sodium pentobarbital (30 mg/kg, i.p.) or a combination of sodium pentobarbital and ketamine hydrochloride (i.m.) and were maintained at a surgical level of anesthesia with an intravenous infusion of sodium pentobarbital in lactated ringer solution. Atropine (1 mg, i.m.) was given to reduce fluid accumulation in the lungs, and we used dexamethasone sodium phosphate (0.14 mg/kg) to prevent brain edema. Local anesthetic was used to treat pressure points and wounds. Body temperature was maintained at 37.5°C with a thermostatically regulated heating pad. The duration of the cortical mapping experiments was between 36 hours and 48 hours. After the induction of anesthesia, the animal's head was immobilized in a custom-made head holder designed to leave the ear canals unobstructed. The external meatae were resected bilaterally and cleared of tissue; then, both pinnae were reflected anteriorly. The auditory cortex, located

within the middle ectosylvian gyrus, was exposed by partial craniotomy and the dura mater removed. To prevent drying, silicone oil was applied to the cortical surface immediately after exposure. The surface of the cortex was then photographed.

The frequency organization of AI was established by conventional microelectrode mapping techniques. All cortical mapping experiments were carried out in an electrically shielded, sound attenuating room. Acoustic stimuli were delivered through a closed, calibrated system (earphone with flexible tubing inserted into the external meatus); the transducer bandwidth ranged from 100 Hz to 40 kHz. Tone stimuli were generated by a frequency synthesizer shaped to a 80-msec duration with 10 msec rise/fall times and presented at a rate of 1–2 per second. Tungsten microelectrodes (1–4 mOhm impedance) were used to record (extracellularly) cortical neuron cluster and single-unit responses to tone-burst stimuli. The electrode was advanced into the cortex by a microdrive and stepping motor. Multiple penetrations were made normal to the cortical surface. The microelectrode signal was amplified, filtered (PBA-1; Frederick Haer Company) and monitored on an oscilloscope and loudspeaker. The signal was passed through a voltage discriminator (window discriminator; Frederick Haer Company) and input to a D/D interface (Cambridge Electronic Design 1401) hosted by an 80286 microcomputer to log all event times (stimulus and spike). During the experiment, the location of each microelectrode penetration was marked on a photograph of the cortical surface. At each electrode position, the characteristic frequency (CF) of the cluster or single unit was determined. Neural responses were collected using an automated procedure under computer control. Tone stimuli were presented in a pseudorandom order from a matrix of different frequency/intensity combinations, and raster displays were constructed.

Retrograde tracers

Retrograde tracers were introduced into different regions of AI using glass micropipettes. The tracers used were 1) wheat germ agglutinin conjugated to horseradish peroxidase (HRP; crystals), 2) nuclear yellow (NY; crystals), 3) Fast Blue (FB; 3%), and 4) FluoroGold (FG; 1%). In each AI field, up to three different tracers were used. HRP and NY were implanted in crystalline form (Mori et al., 1980) at the time of the acute electrophysiological mapping experiment (survival time, 36–40 hours). Injections of FB and FG were carried out during chronic surgery 19 days prior to the acute mapping experiment. In each case, the injection site was mapped relative to cortical landmarks for later superimposition onto the AI frequency map.

At the end of the cortical recording experiment, animals were deeply anaesthetized with an additional dose of sodium pentobarbital (65 mg/kg, i.p.), and intracardiac perfusion was performed with saline, followed by fixative (0.5% glutaraldehyde and 2% paraformaldehyde in 0.1 M phosphate buffer, pH 7.4), and finally with 10% sucrose. The brain was removed and immersed in a series of 10%, 20%, and 30% sucrose solutions in phosphate buffer for cryoprotection. Serial frozen sections (frontal sections; 50 μm) were collected, and alternate sections were either processed by the tetramethylbenzidine (TMB) method for detection of HRP (Mesulam, 1982) or mounted for fluorescence microscopy. Alternate TMB-processed sections (every fourth section) were counterstained with neutral red. All sections were then dehydrated through xylene and coverslipped with Permount (TMB) or Krystalon (fluorescent).

The MGB was assessed for the occurrence of labeled cells using brightfield and fluorescence microscopy. Images were obtained with an Optronics V1470 camera and a Truevision Bravado frame grabber and were processed in Photoshop software (Adobe Systems, Mountain View, CA). Labeled cells were marked on a tracing of the section using a drawing attachment. The location of relevant structures within the thalamus was determined by superimposing the tracings of counterstained neutral red sections with adjacent sections containing labeled cells. Parcellation of the MGB into ventral (MGBv), medial (MGBm), and dorsal (MGBd) divisions was according to the scheme devised by Morest (1964, 1965) and has been used in previous physiological and anatomical studies of the MGB (Imig and Morel, 1984, 1985; Morel and Imig, 1987; Brandner and Redies, 1990; He and Hashikawa, 1998).

RESULTS

Normal control cats

The pattern of thalamocortical connections was studied in four normal cats by injecting HRP and/or fluorescent tracers into different regions of AI. A typical example of the results is shown in Figure 1. The AI area is located on the temporal gyrus and is bounded approximately by the anterior ectosylvian fissure (AEF) and the posterior ectosylvian fissure (PEF), as shown on the bottom right in Figure 1. Within AI, sound frequencies are represented in an orderly fashion, reflecting the frequency-place code within the cochlea (cochleotopic or tonotopic organization). Neurons that respond best to low-frequency acoustic stimuli represent the cochlear apex and are located posteriorly, whereas those that are activated best by high-frequency stimuli and that derive input from the base of the cochlea are positioned anteriorly. Isofrequency contours have been superimposed at octave intervals. In general, these contours tend to run in the dorsal-ventral plane.

The positions of retrograde tracer injections are indicated on the tonotopic map in Figure 1 by the star and the inverted triangle symbols for FG and NY, respectively, together with the histologically determined diffusion zone around the injection point. Labeling sites in the MGB are illustrated in four sections that were 200 μm apart. AI receives thalamocortical projections from separate medial and lateral arrays or columns in the auditory thalamus (Andersen et al., 1980; Merzenich et al., 1982; Middlebrooks and Zook, 1983; Brandner and Redies, 1990). Our experiments reveal that labeling is most extensive in the lateral array located in the MGBv. In general, this lateral array appears as a dorsoventrally oriented band rostrally that folds medially and subdivides into dorsal and ventral components farther caudally. Additional discontinuities in the lateral array were also observed in some cases. In Figure 1, this pattern of retrograde labeling can be seen in the lateral arrays located in MGBv.

The location and precise topographic pattern of labeling in MGBv varied as a function of injection site location along the cochleotopic (anterior-posterior) axis in AI. In

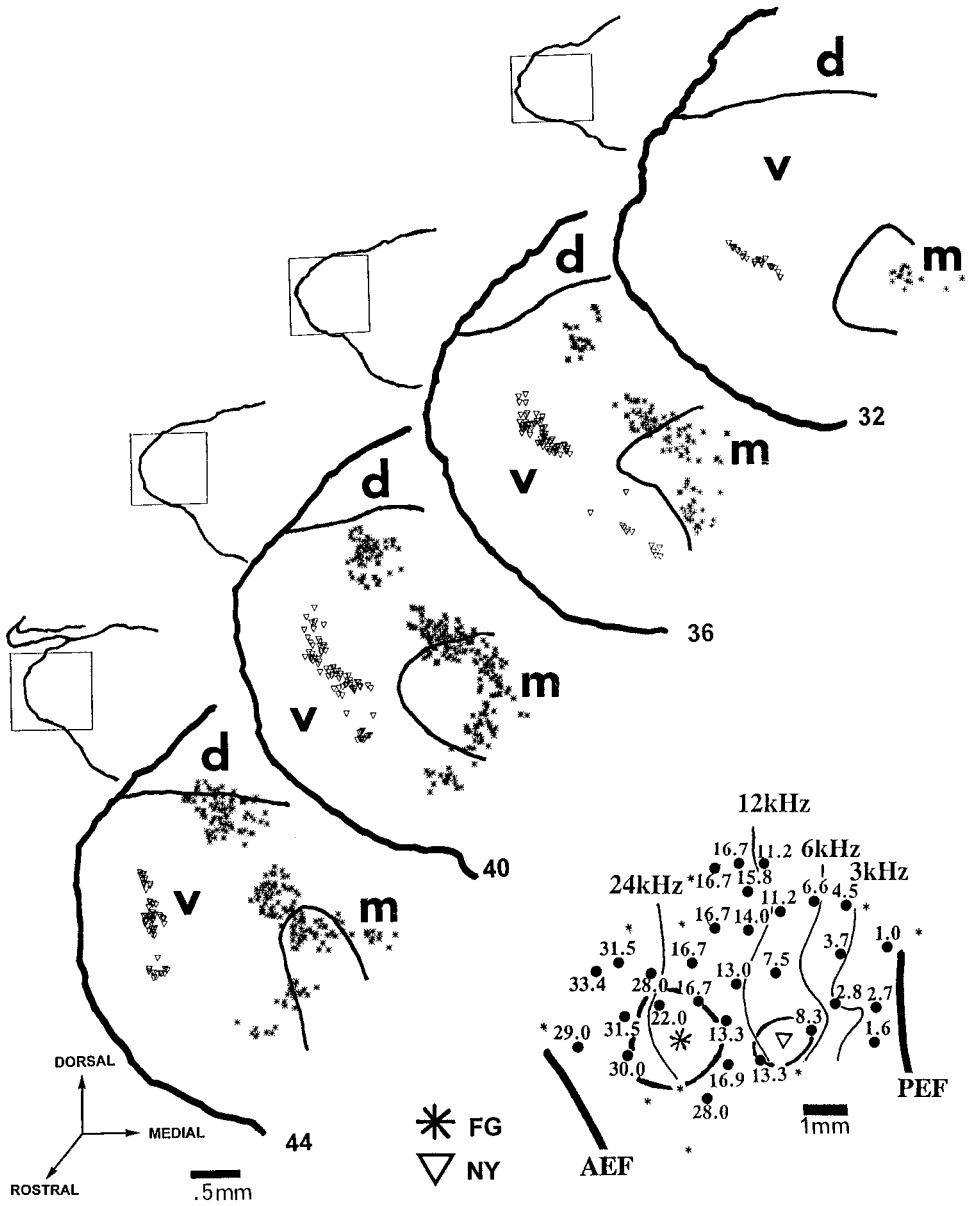

Fig. 1. Auditory thalamocortical pathways of a normal adult cat. Frequency map of the primary auditory cortex (AI; bottom right) based on neuron characteristic frequency (CF; in kHz) with isofrequency contours marked at octave intervals. AEF, anterior ectosylvian fissure; PEF, posterior ectosylvian fissure. Injection sites of FluoroGold (FG; star) and nuclear yellow (NY; triangle) are shown together with diffusion zones. The main drawing shows four sections 200 μm apart through the medial geniculate nucleus with dorsal (d), ventral (v), and medial (m) subareas indicated. Cells labeled with FG or NY are shown.

the example shown in Figure 1 and in another control animal that also received two different tracer injections in AI, when the injection sites do not overlap, a completely separate array of cells in MGBv is labeled by each neural tracer. These two bands of labeled neurons were spatially segregated, thus forming two rather than one lateral array of labeled cells. The FG-labeled cells in MGBv, as illustrated in Figure 1, are situated medially when the injection site (FG) is located in a more anterior (high-frequency CF) region of AI; this band of labeled cells folds around the more lateral band of cells labeled by a second tracer injection (NY) into the posterior (low-frequency CF) region of AI.

Experimentally treated subjects

In Figures 2–6, the results from animals with amikacin-induced neonatal cochlear damage are presented. All of the treated cats exhibited substantial ABR threshold elevations and abnormal maps of frequency representation in AI. In each case, ABR thresholds to high-frequency stimuli were elevated, indicating a severe high-frequency hearing loss. The degree of residual, low-frequency hearing varied between subjects. Tonotopic maps in AI demonstrate a dramatic departure from the normal pattern of cochleotopic representation. The most obvious feature of the cortical organization in each of these cats is the over-

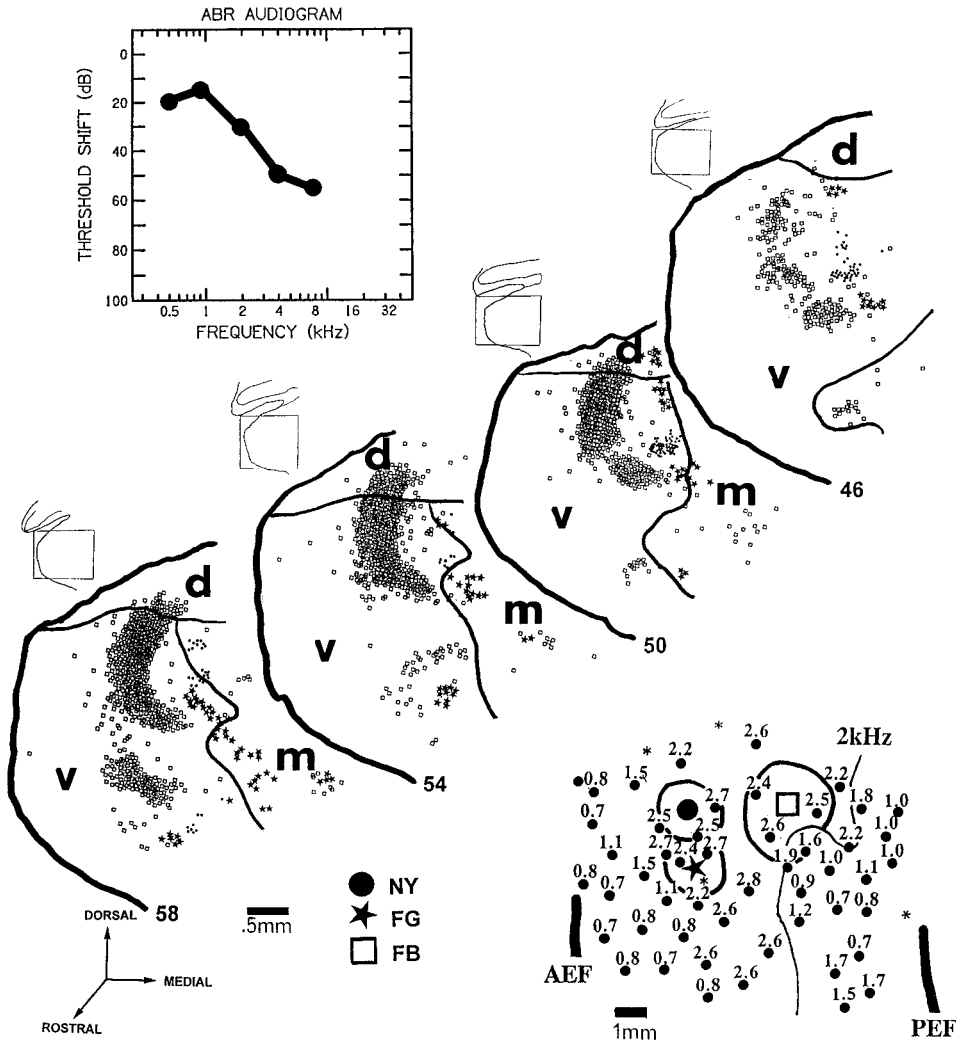

Fig. 2. Auditory thalamocortical pathways in adult cat after neonatally induced basal cochlear lesion. The top left graph is an auditory brainstem response (ABR) audiogram. The bottom right shows the characteristic frequency (CF)-based (in kHz) tonotopic map of AI cortex with the 2-kHz isofrequency contour marked. AEF, anterior ectosylvian fissure; PEF, posterior ectosylvian fissure. Injection sites of NY (solid circle), FG (star), and fast blue (FB; open square) are indicated together with limits of diffusion zones. The main central drawings show four sections from the medial geniculate nucleus with dorsal (d), ventral (v), and medial (m) regions indicated. Cells labeled with NY, FG, and FB are shown.

representation of neurons tuned to a restricted range of stimulus frequencies.

Generally, we can note that retrograde tracer experiments reveal lateral and medial arrays of labeled neurons in MGB in all our amikacin-treated cats. Like in the normal control animals, labeling in the neonatally deafened cats was most extensive in the lateral arrays, indicating that the major input to AI originates in the MGBv. In each case, labeled cells of the lateral array formed narrow, dorsoventral bands in rostral MGBv that folded and separated into clusters farther caudally. Fewer labeled cells were found in the medial array located rostrally in posterior thalamus and farther caudally in MGBd and MGBm.

For the cat shown in Figure 2, the ABR audiogram shows a mild, 10–20 dB ABR threshold loss at frequencies around 1 kHz and below and a high-frequency hearing loss above 1 kHz with a steep slope to the audiogram. In the AI map, characteristic frequencies ranged from 0.7 kHz to 2.7 kHz. Although a low- to high-frequency progression along the posterior-anterior axis was present, the cochleotopic organization below 2 kHz appears distorted. The most abnormal feature of this map is the expansion of the area containing neurons tuned to between 2 kHz and 3 kHz in the anterior portion of AI. This overrepresentation of the 2–3 kHz region corresponds to the steep slope of the ABR audiogram at the same frequencies and, thus, to the edge of the cochlear lesion. This amikacin-treated cat was given multiple fluorescent tracer injections in AI, as shown in Figure 2. FB (Fig. 2, open square) was injected at a central position in AI, whereas NY (Fig. 2, solid circle) and FG (Fig. 2, star) were placed at a more anterior site in AI but were aligned along the same dorsal-ventral axis. A photomicrograph of the cortical injection site is shown on

the top in Figure 3, providing an indication of the diffusion zone around each injection site and, thus, the degree of separation between labeled areas. In a normal cat, these tracers would be associated with high-frequency (NY and FG) and middle frequency (FB) positions in the AI cochleotopic map. However, due to the abnormal cochleotopic map in this deafened cat, all tracers were approximately located in the 2.5-kHz region. Despite this altered cortical frequency representation, the pattern of labeling in MGBv was similar to that of the controls. In Figure 2, representative sections from the rostrocaudal series illustrate the pattern of labeling for all three tracers in the middle one-third of the MGBv. The FB injection into central AI produced a dorsoventrally oriented band of labeled cells rostrally that then folded and divided into dorsal and ventral components farther caudally in the MGBv. The NY and FG injections into anterior AI together produced an elongated array of cells medial and ventral to the FB-labeled area of MGBv. However, the NY- and FG-labeled cells in the MGBv were not randomly intermingled. In AI, the NY injection site was positioned at the same anterior location but dorsal to the FG site; in MGBv, these two tracers produced segregated cell clusters. Specifically, the NY- and FG-labeled cells were arranged in a dorsoventral sequence of alternating clusters that, together, formed a band that folded medially in section 58. This array then separated into dorsal and ventral components farther caudally, with both FG and NY clusters in the dorsal component and FG-labeled cells only in the ventral component. Small numbers of FB-labeled cells were randomly distributed around the main FB clusters; most occurred in isolated positions, whereas a few were intermingled with the NY and FG patches. A "raw data" photomicrograph of section 48 from this cat is shown on the bottom in Figure 3. Note how the separate tracers are easily distinguished even at this low magnification.

For the three cats illustrated in Figures 4–6, there was more extensive damage to the cochlea, as indicated by the greater elevation of the ABR thresholds. The AI map of the subject in Figure 4 exhibits CFs from 0.6 kHz to 1.7 kHz, and the typical frequency progression is absent. A similar disruption of the cochleotopic order in AI is observed in the cat in Figure 5, in which the cortical map contains neurons with CFs limited to between 0.4 kHz and 1.3 kHz. Figure 6 illustrates the subject with the most severe low-frequency hearing loss, with ABR threshold elevations of 30 dB or more below 4 kHz. Again, the cortical frequency map is clearly abnormal, with no representation of frequencies above 1.2 kHz. In all of these animals with elevated low-frequency ABR thresholds, the basic cochleotopic organization seems to be absent even in the posterior (low-frequency) area of AI.

In each of these three cats (Figs. 3–6), HRP was injected into the posterior region of AI, whereas NY was placed at a more anterior location. Under normal circumstances, HRP would have been in a low-frequency position of the AI map, and NY would have been at a middle- to high-frequency position. The pattern of labeling in the MGB suggests that the topography of the thalamocortical projection was normal, despite the abnormal frequency organization in AI. In each case, NY and HRP formed segregated populations of labeled cells in the MGBv. The correlation between the injection sites in AI and the location of labeled cells in MGB was similar to that described above for the amikacin-treated cat in Figure 2 and for the control group (exemplified in Fig. 1). In each case, the HRP population (posterior AI injection site) was positioned lateral to the NY-labeled array (anterior AI injection site) in the MGBv. The topography of the HRP-labeled array in each of these amikacin-treated cats is as expected for neural tracer injections into a posterior, normally low-frequency region of AI. The HRP-labeled cells in the rostral MGBv formed a vertical sheet (see, e.g., Fig. 5, section 53; Fig. 6, section 59). In the middle one-third of the MGBv, there was a horizontal extension of the array or a medial cluster of labeled cells (see, e.g., Fig. 4, sections 43–55; Fig. 5, sections 41–45; Fig. 6, sections 47–55). A reduction of the ventral component occurred in the most caudal aspect of the array (see Fig. 5, section 41 and Fig. 6, section 47). The HRP array in most sections was not a continuous sheet but, instead, was composed of clusters of labeled cells.

Now, consider the topography of the NY-labeled areas. In each amikacin-treated cat, NY was placed in a more anterior position in AI compared with HRP, a region that, in normal hearing cats, would represent the middle- to high-frequency range of CF. In the middle one-third of the MGBv, dorsal and ventral components appear and are separated by a region that is devoid of NY-labeled cells. Figure 5 (sections 41 and 45) and Figure 6 (sections 47 and 51) show that the NY-labeled dorsal and ventral components are further segregated into discontinuous clusters. In each case, the NY-labeled dorsal and ventral components are intersected by a medial cluster of HRP-labeled cells (see, e.g., Fig. 4, sections 47 and 48; Fig. 5, section 45; Fig. 6, sections 51 and 55). This portion of the HRP-labeled array is the horizontal extension described above that, in some cases, lies within the void or "hole" in the NY array. These dorsal and ventral components then merge into a single, dorsoventrally labeled band in the rostral one-third of the MGBv (Fig. 5, section 53; Fig. 6, section 59).

In summary, tracer injections into AI produced a pattern of retrograde labeling in the auditory thalamus of the amikacin-treated cats similar to that found in the normal control group. Labeling was most extensive in the lateral array or column located in the MGBv; each injection of tracer into AI produced a dorsoventrally oriented, folded sheet of labeled cells. The pattern of labeling varied systematically with the location of the tracer injection site in AI. Thus, anterior AI injections produced labeled cells in the lateral MGBv, and posterior AI injections labeled more medially in the MGBv. When multiple tracers were used in the same subject and the injection sites in AI did not overlap, these different tracers labeled spatially segregated bands of cells in the MGBv in both deafened animals and control animals. These results demonstrate that, despite the abnormal maps in AI, the topographic pattern of labeling in the auditory thalamus was normal in our neonatally deafened cats.

DISCUSSION

Thalamocortical pathways

Combined retrograde tracer and electrophysiological mapping techniques have previously shown that, in normal cats, thalamic neurons of a similar CF are organized into segregated bands or laminae in MGBv and, in turn, innervate a corresponding cortical region of the same characteristic (Andersen et al., 1980; Merzenich et al.,

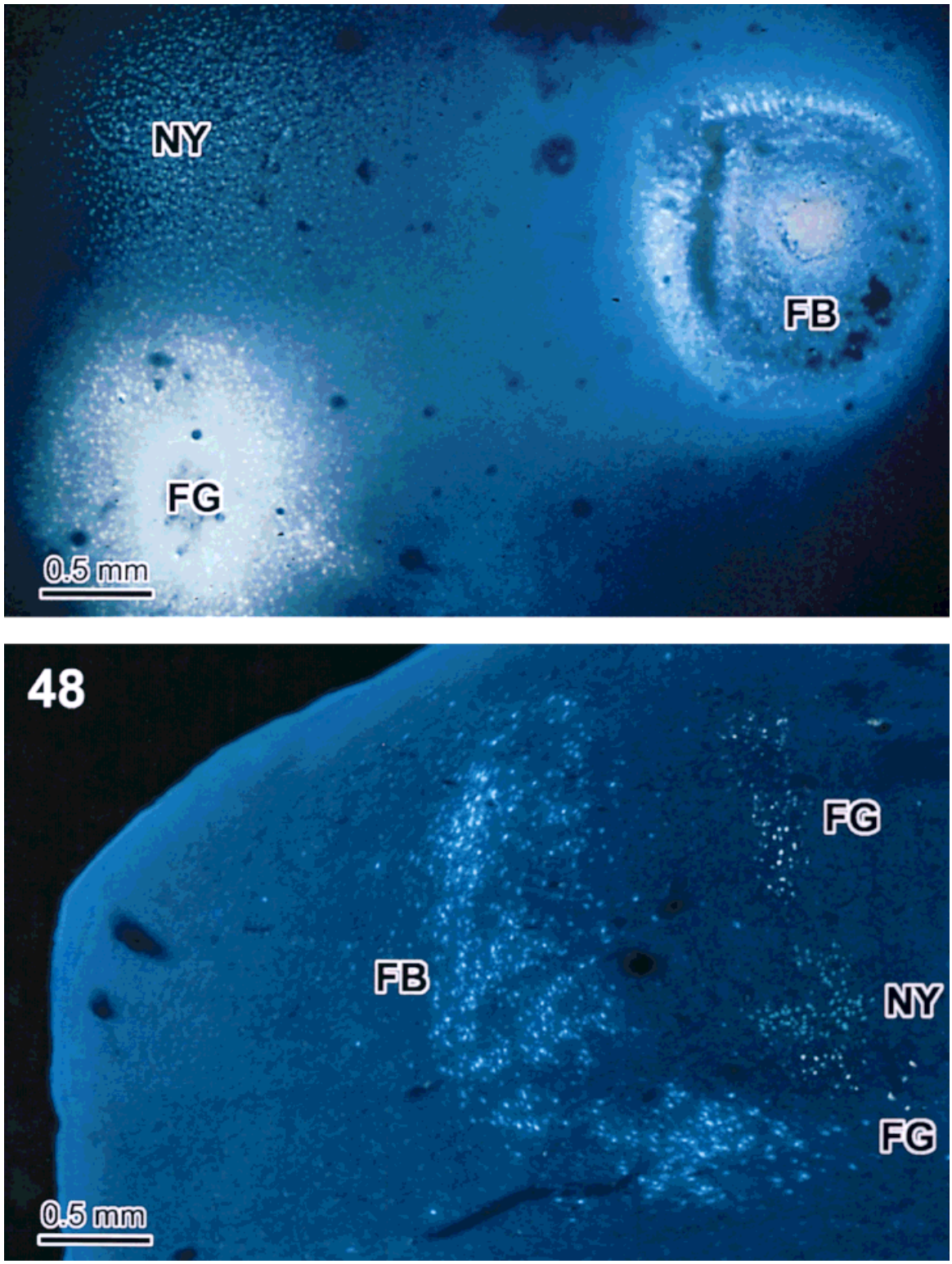

Fig. 3. Ultraviolet fluorescence photomicrographs from the cat shown in Figure 2. **Top:** The injection sites at the level of the primary auditory cortex. **Bottom:** Labeled cells in one section (no. 48) through the medial geniculate nucleus.

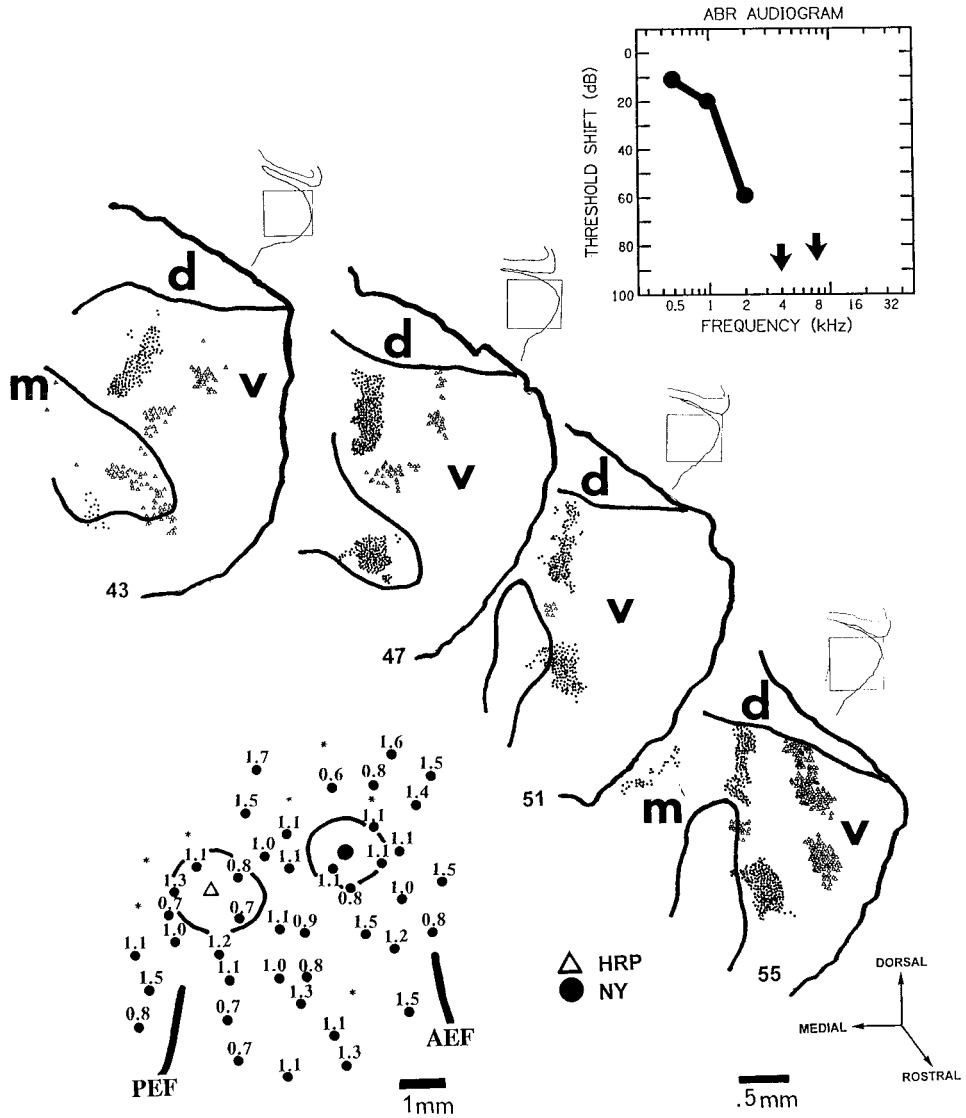

Fig. 4. Thalamocortical pathway tracing in adult cat after neonatal cochlear lesion. The top right graph is an ABR audiogram. The bottom left shows cortical tonotopic map (CFs in kHz). AEF, anterior ectosylvian fissure; PEF, posterior ectosylvian fissure. Injection sites of horseradish peroxidase (HRP; open triangle) and NY (solid circle) are shown with local diffusion zones. The central drawings show four sections from the medial geniculate body (MGB) with dorsal (d), ventral (v), and medial (m) regions and tracer-labeled cells indicated.

1982; Imig and Morel, 1983, 1984, 1985; Middlebrooks and Zook, 1983; Winer, 1985; Morel and Imig, 1987). For each neural tracer, the thalamic arrays of labeled cells form separate, elongated lamina in MGBv. These labeled neurons cluster into patches or bands with similarly labeled cells to form these segregated lamina. Merzenich et al. (1982) described one cat that received two injections of the same retrograde tracer at different frequency locations along the anteroposterior axis in AI. The results of that experiment revealed two clearly separate bands of labeling: one located medially in MGBv and the other located more laterally. Both arrays formed dorsoventral lamina in the rostral MGBv, then folded medially farther caudally, a topography similar to that found in our subjects. Brandner and Redies (1990) also reported that labeled cell populations in the MGB did not overlap when multiple AI tracer injections were placed along the anteroposterior axis of AI, but no data were presented.

A topographical pattern of connections between MGB and AI may exist not only across the frequency dimension but also within the projection associated with a single isofrequency contour. Evidence from previous anterograde and retrograde tracer studies reveal clustered, "patchy" connections between the MGBv and the AI. These patches are distributed in a pattern aligned with the orientation of isofrequency contours in AI and MGBv (Andersen et al., 1980; Merzenich et al., 1982; McMullen and deVenecia, 1993; deVenecia and McMullen, 1994). However, other details relating to the complexity of this topographic pattern of thalamocortical connections between isofrequency bands of similar CF (individual variation in rostral/caudal and local gradients, differences associated with CF, and

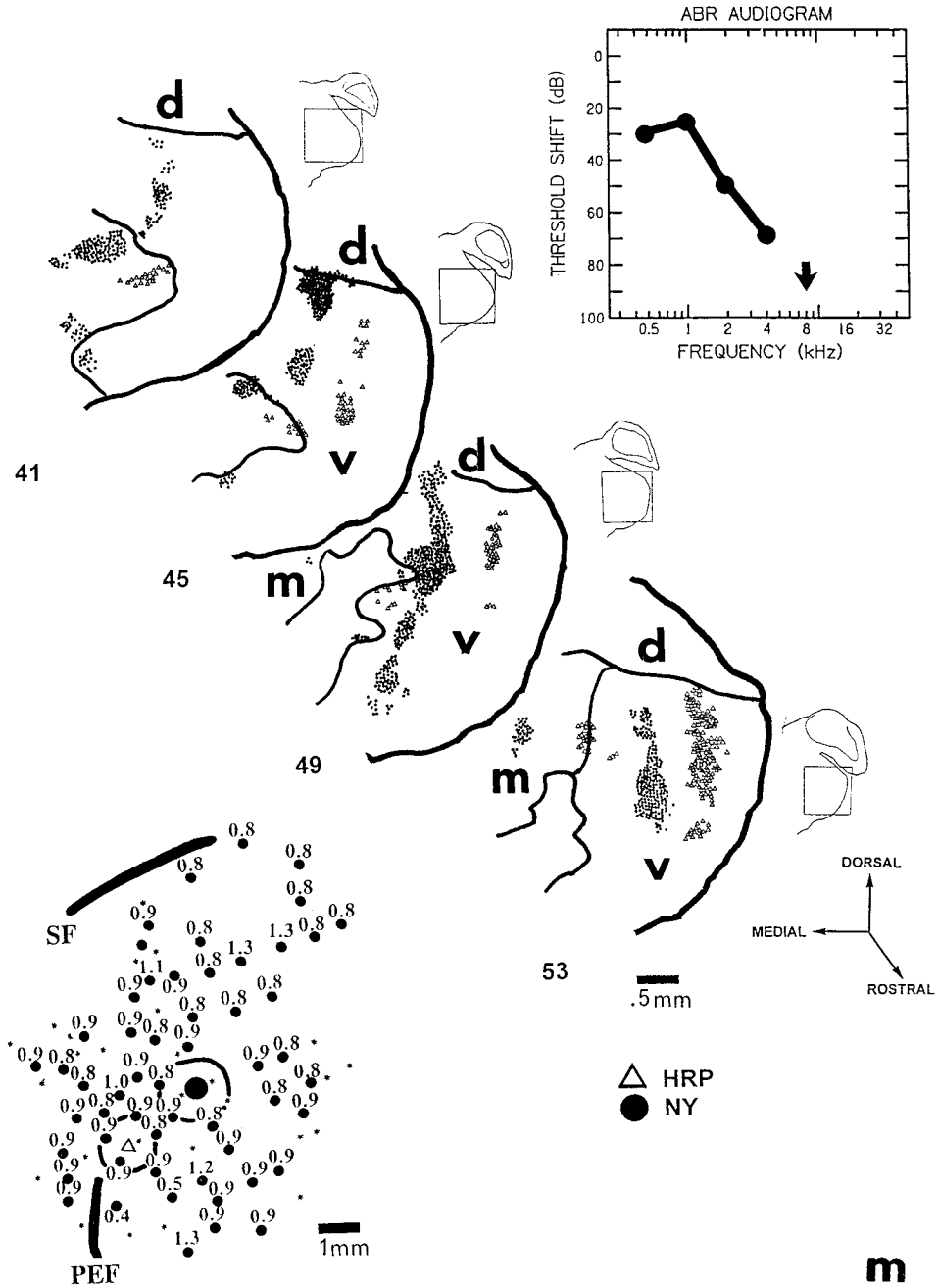

Fig. 5. Thalamocortical pathways in adult cat after neonatal cochlear lesion. The functional state of the auditory system is indicated by the ABR audiogram (top right). The cochleotopic map in primary auditory cortex (CFs in kHz) is shown on the bottom left with the injection sites and diffusion zones for HRP (open triangle) and NY (solid circle) indicated. AEF, anterior ectosylvian fissure; SF, sylvian fissure. Four representative sections through the MGB are shown with dorsal (d), ventral (v), and medial (m) regions indicated and with all sites of tracer-labeled cells shown.

extent of divergence/convergence; functional significance) require further investigation (Middlebrooks and Zook, 1983; Brandner and Redies, 1990; Winer et al., 1999). Nevertheless, a common finding in the retrograde neural tracer studies was that, with small tracer injections into AI, the labeled cells in MGBv are segregated into clusters rather than forming a solid, dorsoventrally oriented array of labeled cells (Andersen et al., 1980; Merzenich et al., 1982; Middlebrooks and Zook, 1983). In our study, a similar pattern of labeling was observed, with cell arrays often arranged into several bands and clusters within the dorsoventrally oriented and folded arrays; this was the case for both the normal animals and the amikacin-treated animals. In the amikacin-treated cat shown in Figure 2, two different tracers (FG and NY) at different dorsoventral positions in the anterior AI labeled separate,

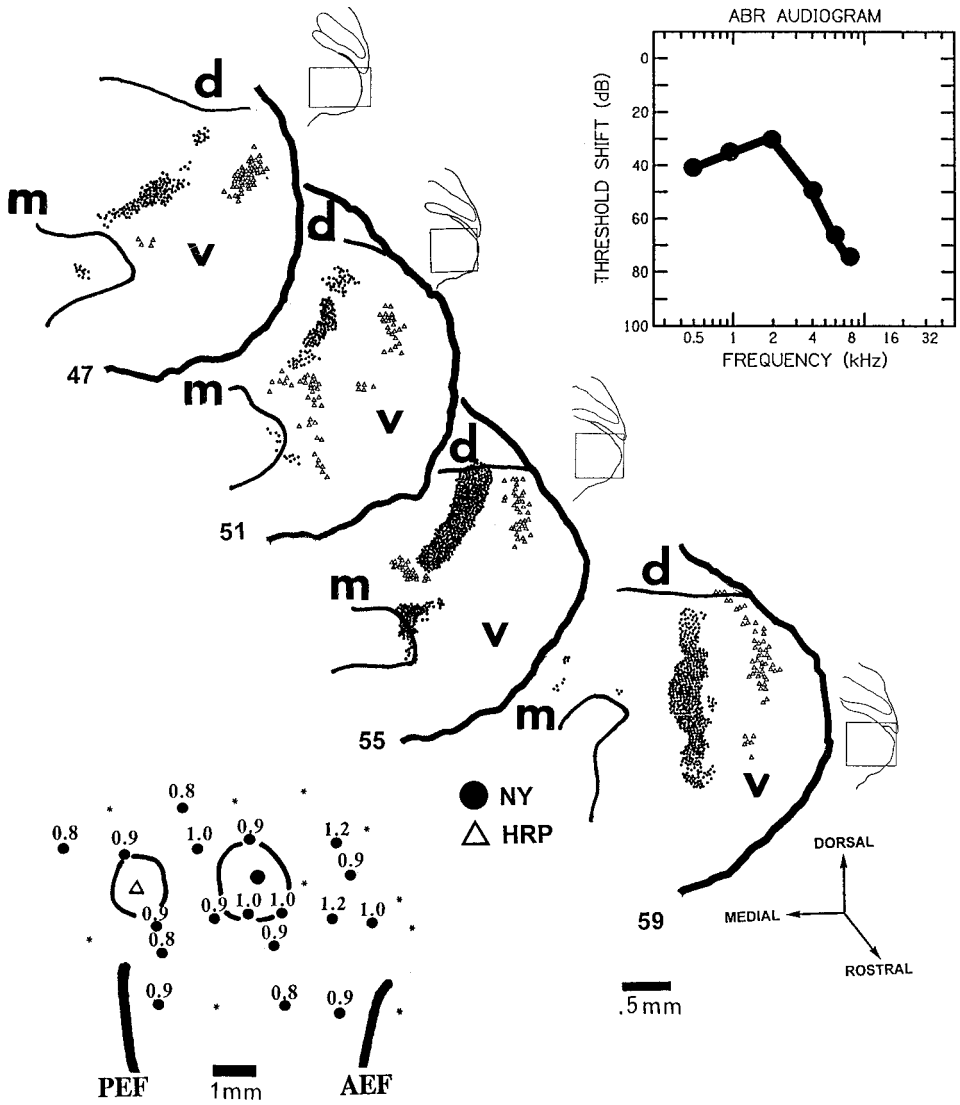

Fig. 6. Thalamocortical pathways in adult cat after neonatal cochlear lesion. The top right graph shows an ABR audiogram. The cochleotopic map in primary auditory cortex (CFs in kHz) is in the bottom left with the injection sites and diffusion zones for HRP (open triangle) and NY (solid circle) shown. AEF, anterior ectosylvian fissure; PEF, posterior ectosylvian fissure. Four representative sections through the MGB are shown with dorsal (d), ventral (v), and medial (m) regions indicated and with all sites of tracer-labeled cells shown.

alternating cell clusters within the same dorsoventrally oriented array in the MGBv. This general finding of segregated labeling is similar to that reported by others using multiple retrograde tracers injected at different dorsoventral locations in the AI (Middlebrooks and Zook, 1983; Brandner and Redies, 1990). In this study, binaural response properties were not mapped in AI, and the relationship between the functional significance and the topography of thalamocortical connections within the isofrequency domain cannot be addressed. Further studies examining the detailed topography of thalamocortical connections within isofrequency laminae are necessary to determine whether the pattern of connections within the isofrequency dimension is maintained despite neonatally induced hearing loss.

Thalamocortical connections after AI reorganization

The development and maintenance of the spatial representation of sound frequency (cochleotopic/tonotopic maps) in AI appear to depend on normal levels of excitation of the auditory periphery. Damage to the cochlear sensory epithelium can disrupt the organization of these cortical maps in the adult subject (Robertson and Irvine, 1989; Rajan et al., 1993) and, perhaps more substantially, when peripheral lesions are made during early postnatal development (Harrison et al., 1991). In this study, we examined the consequences of neonatal cochlear lesions with a focus on the relationship between the cochleotopic organization of AI and the topography of thalamocortical

connections between the ventral division of the MGB and AI.

Our electrophysiological mapping experiments demonstrate that an abnormal cochleotopic representation develops in the auditory cortex as a consequence of partial deafferentation, resulting from ototoxic cochlear damage in newborn kittens. In this paper, we use the ABR audiogram (ABR thresholds to tone pip stimuli) to represent the functional condition of the cochlea after amikacin-induced lesions. The ABR thresholds quite accurately reflect the integrity of the cochlear sensory epithelium, as we have previously shown in amikacin-treated kittens (Mount et al., 1991; Harrison et al., 1993a). Thus, in the ABR audiograms of the cats in the present study, threshold shifts $>$ 55 dB are associated with a total loss of inner and outer hair cells and, thus, a cochlear deafferentation in that region. ABR threshold elevations $>$ 15 dB reliably indicate a partial loss of cochlear hair cells that is likely to result in a reduced amount of cochlear afferent activity compared with that arising from an intact region of the cochlea. In amikacin-treated kittens, ABR thresholds within 15 dB of normal are almost always indicative of an intact cochlear sensory epithelium (Mount et al., 1991)

For each of the amikacin-treated cats presented here, the AI frequency map is characterized by an overrepresentation of a restricted CF range. For example, the cortical map of the amikacin-treated cat of Figure 2 exhibits an expanded representation of the 2–3 kHz range, corresponding to the high-frequency, cut-off slope of the ABR audiogram that, in turn, corresponds with the boundary of the cochlear lesion. This "expanded" section of the cortical map occupies the region of auditory cortex that would normally represent the "missing" cochlear input. In the other three experimental cats (Figs. 4–6), the organization of low-frequency representation in the posterior region of AI appears to reflect the status of the cochlea in the apical turn. When low-frequency ABR thresholds are normal, the posterior area of cortex usually exhibits a relatively normal representation of low-frequency sound (Harrison et al., 1991). However, in these three amikacin-treated cats (Figs. 4–6) with more severe deficits (as reflected in greater ABR threshold elevations), the entire AI map is limited to the representation of frequencies below 2 kHz, with no apparent cochleotopic order. For these animals with greater functional deficits, the reduction of ascending input appears to prevent the development of a normal cortical representation even in the low-frequency regions of the AI map.

In the neonatally deafened group, the extent of expanded cortical representation was up to 5 mm in some cases. This expansion is considerably greater than the previously reported reorganization of auditory cortex in adult animals (Robertson and Irvine, 1989; Rajan et al., 1993; Schwaber et al., 1993). Similar but less extensive expansions of cortical representation, previously observed in adult sensory systems, were thought to occur within the normal spread of thalamocortical afferents in cortex (Kaas et al., 1983; Merzenich et al., 1984; Robertson and Irvine, 1989; Gilbert and Wiesel, 1992; Schwaber et al., 1993). Because the potential for morphologic change is greater during the neonatal period (Shatz and Stryker, 1978; Pidoux et al., 1979, 1980; LeVay et al., 1980; Swindale, 1981; Jeffrey, 1984b; Shook and Chalupa, 1986; Stryker and Harris, 1986; Trevalyan and Thompson, 1992), we hypothesized that changes in the organization of the thalamocortical projection might account for the massive expansions that develop in the cortical maps of our neonatally lesioned animals. However, the results of the present study do not support this hypothesis; the normal pattern of segregated, cochleotopically organized connections is still present in the thalamocortical projection despite the altered physiological organization of the cortical frequency map in the neonatally deafened cats. Our results concur with those described for digit-amputation studies in the adult raccoon that also found that expansions in somatosensory cortex were not accompanied by a change in the thalamocortical projection (Rasmusson and Nance, 1986).

A number of important questions arise from this work. First, at which level(s) within the auditory pathway does the reorganization of cochleotopic maps that we observe occur? Second, what are the differences between adult plasticity (i.e., map reorganization induced in the mature animal) and developmental plasticity (changes resulting from peripheral lesions made during early postnatal development)? The question of where reorganization occurs was central to the initiation of these studies. If the cochleotopic map reorganization was within the cortex, then the patterns of thalamocortical projections would be considerably different from those that we observed. The clear point-to-point connections that we report mean that cochleotopic maps at the thalamic level are similarly reorganized. With regard to lower levels, no studies have been reported so far in the cat at subthalamic levels. However, essentially the same experiments have been carried out in the chinchilla in which cochleotopic map changes in the inferior colliculus (central nucleus) have been observed after neonatal cochlear lesions (Harrison et al., 1996, 1998). The midbrain reorganization observed is similar with respect to the extent of the overrepresentation of a frequency region related to the boundary of the cochlear lesion. We also note that partially damaged cochlear areas give rise to abnormally organized maps. These findings support previous work by Willott (1984) in presbyacusic mice. Therefore, we can confidently suppose that the reorganization that we observe in the present study at the level of auditory cortex is, in large measure, a reflection of changes at the midbrain level. Furthermore, although there is no direct evidence to date, it is logical to hypothesize that, in a developmental plasticity model, where ever there are synapses, there is potential for reorganization based on synaptogenesis and synaptic strengthening. Thus, one could speculate that, at the brainstem level and even at the cochlea, reorganization is feasible.

Most of the seminal studies on cochleotopic map reorganization were done in the adult animal at the cortical level (see, e.g., Robertson and Irvine, 1989; Rajan et al., 1993). Implicit in the discussion of these studies was the notion that the reorganization observed was cortical or perhaps thalamocortical. Later adult plasticity studies have determined that there is no real plasticity at the level of the cochlear nucleus (Kaltenbach et al., 1992, 1996). We have preliminary data (unpublished) to suggest that there is very little reorganization (in terms of expanded frequency representation) in the inferior colliculus of the chinchilla after cochlear lesions in the adult animal. Thus, we can tentatively suggest that adult plasticity is largely the result of high-level changes, primarily at the thalamocortical level. However, given the intimacy of ascending and descending fibers at all levels in the auditory

pathway, one should not expect a find an absolute boundary in this regard.

Finally it is important to mention that this work on cochleotopic map reorganization in animal models bears directly on the developmental consequences of long-term cochlear hearing loss in children. Thus, the amikacin-treated kittens in the present study are directly equivalent to an infant with a high-frequency sensorineral hearing loss. In this regard, the ABR audiograms that we use to characterize the functional deficits in our kittens are closely related (±12 dB) to behavioral audiograms (Harrison et al., 1992). The cochleotopic map abnormalities that we report here, as well as the thalamocortical connection patterns, are likely to have strong cross-species analogies.

LITERATURE CITED

Andersen RA, Knight PL, Merzenich MM. 1980. The thalamocortical and corticothalamic connections of AI, AII and the anterior auditory field (AAF) in the cat: evidence for two largely segregated systems of connections. J Comp Neurol 194:663–701.

Brandner S, Redies H. 1990. The projection from medial geniculate to field AI in cat: organization in the isofrequency dimension. J Neurosci 10: 50–61.

Brugge JF. 1983. Development of lower brainstem auditory nuclei In: Romand R, editor. Development of auditory and vestibular systems. New York: Academic Press. p 89–120.

Brugge JF. 1988. Stimulus coding in the developing auditory system. In: Edelman GM, Gall WE, Cowan WM, editors. Auditory function: neurobiological bases of hearing. New York: John Wiley & Sons. p 113–136.

Carlier E, Lenoir M, Pujol R. 1979. Development of cochlear frequency selectivity tested by compound action potential tuning curves. Hearing Res 1:197–201.

de Venecia RK, McMullen NT. 1994. Single thalamocortical axons diverge to multiple patches in neonatal auditory cortex. Brain Res Dev Brain Res 81:135–142.

Ehret G. 1985. Behavioural studies on auditory development in mammals in relation to higher nervous system functioning Acta Otolaryngol (Stockholm) 421(Suppl):31–40.

Ehret G, Romand R. 1981. Postnatal development of absolute auditory thresholds in kittens. J Comp Physiol Psychol 95:304–311.

Gilbert CD, Wiesel TN. 1992. Receptive field dynamics in adult primary visual cortex. Nature 356:150–152.

Harrison RV, Nagasawa A, Smith DW, Stanton SG, Mount RJ. 1991. Reorganization of auditory cortex after neonatal high frequency cochlear hearing loss. Hearing Res 54:11–19.

Harrison RV, Smith DW, Nagasawa A, Stanton SG, Mount RJ. 1992. Developmental plasticity of auditory cortex in cochlear hearing loss: physiological and psychophysical findings. Adv Biosci 83:625–633.

Harrison RV, Stanton SG, Nagasawa A, Ibrahim D, Mount RJ. 1993a. The effects of long-term cochlear hearing loss on the functional organization of the central auditory pathways. J Otolaryngol 22:4–11.

Harrison RV, Stanton SG, Ibrahim D, Nagasawa A., Mount RJ. 1993b. Neonatal cochlear hearing loss results in developmental abnormalities of the central auditory pathways. Acta Otolaryngol (Stockholm) 113: 296–302.

Harrison RV, Ibrahim D, Stanton SG, Mount RJ. 1996. Reorganization of frequency maps in chinchilla: auditory midbrain after long-term basal cochlear lesions induced at birth. In: Salvi RJ, Henderson D, Fiorino F, Colletti V, editors. Auditory system plasticity and regeneration, scientific and clinical implications. New York: Georg Thieme. p 238–255.

Harrison RV, Ibrahim D, Mount RJ. 1998. Plasticity of tonotopic maps in auditory midbrain following partial cochlear damage in the developing chinchilla. Exp Brain Res 123:449–460.

He J, Hashikawa T. 1998. Connections of the dorsal zone of cat auditory cortex. J Comp Neurol 400:334–348.

Imig TJ, Morel A. 1983. Organization of the thalamocortical auditory system in the cat. Annu Rev Neurosci 6:95–120.

Imig TJ, Morel A. 1984. Topographic and cytoarchitectonic organization of thalamic neurons related to their targets in low, middle and high frequency representations in cat auditory cortex. J Comp Neurol 227: 511–539.

Imig TJ, Morel A. 1985. Tonotopic organization in the ventral nucleus of the medial geniculate body in the cat. J Neurophysiol 53:309–340.

Jeffrey G. 1984a. Retinal ganglion cell death and terminal field retraction in the developing rodent visual system. Brain Res Dev Brain Res 13:81–96.

Jeffrey G. 1984b. Transneuronal effects of early eye removal on geniculocortical projection cells. Brain Res Dev Brain Res 13:257–263.

Kaas JH, Merzenich MM, Killackey HP. 1983. The reorganization of somatosensory cortex following peripheral nerve damage in adult and developing mammals. Annu Rev Neurosci 6:325–356.

Kaltenbach JA, Czaja J, Kaplan CR. 1992. Changes in the tonotopic map of dorsal cochlear nucleus following induction of cochlear lesions by exposure to intense sound. Hearing Res 59:213–223.

Kaltenbach JA, Meleca RJ, Falzarano PR. 1996 Alterations in the tonotopic map of cochlear nucleus following cochlear damage. In: Salvi RJ, Henderson D, Fiorino F, Colletti V, editors. Auditory system plasticity and regeneration, scientific and clinical implications. New York: Georg Thieme. p 317–332.

Kitzes LM. 1984. Some physiological consequences of neonatal cochlear destruction in the inferior colliculus of the gerbil, meriones unguiculatus. Brain Res 306:171–178.

Kitzes LM, Semple MN. 1985. Single-unit responses in the inferior colliculus: effects of neonatal unilateral cochlear ablation. J Neurophysiol 53:1483–1500.

LeVay S, Wiesel TN, Hubel DH. 1980. The development of ocular dominance columns in normal and visually deprived monkeys. J Comp Neurol 191:1–51.

McMullen NT, de Venecia RK. 1993. Thalamocortical patches in auditory neocortex. Brain Res 620:317–322.

Merzenich MM, Colwell SA, Andersen RA. 1982. Auditory forebrain organization, Thalamocortical and corticothalamic connections in the cat. In: Woolsey CN, editor. Cortical sensory organization, multiple auditory areas, vol 3. Clifton, NJ: The Humana Press. p 43–57.

Merzenich MM, Nelson R, Stryker M, Cynader M, Schoppmann A, Zook J. 1984. Somatosensory cortical map changes following digit amputation in adult monkeys. J Comp Neurol 224:591–605.

Mesulam MM. 1982. Tracing neural connections with horseradish peroxidase. New York: John Wiley & Sons.

Middlebrooks JC, Zook JM. 1983. Intrinsic organization of the cat's medial geniculate body identified by projections to binaural response-specific bands in the primary auditory cortex. J Neurosci 3:203–224.

Moore DR. 1985. Postnatal development of the mammalian central auditory system and the neural consequences of auditory deprivation. Acta Otolaryngol (Stockholm) 421(Suppl):19–30.

Moore DR, Kitzes LM. 1985. Projections from the cochlear nucleus to the inferior colliculus in normal and neonatally cochlea-ablated gerbils. J Comp Neurol 240:180–195.

Morel A., Imig TJ. 1987. Thalamic projections to fields A, AI, P and VP in cat auditory cortex. J Comp Neurol 265:119–144.

Morest DK. 1964. The neuronal architecture of the medial geniculate body of the cat. J Anat Lond 98:611–630.

Morest DK. 1965. The laminar structure of the medial geniculate body of the cat. J Anat Lond 99:143–160.

Mori J, Hori N, Katsuda N. 1980. A new method for application of horseradish peroxidase into a restricted area of the brain. Brain Res Bull 6:19–22.

Mount RJ, Harrison RV, Stanton SG, Nagasawa A. 1991. Correlation of cochlear pathology with high frequency hearing loss. Scanning Microsc 5:1105–1113.

Nordeen KW, Killackey HP, Kitzes LM. 1983. Ascending projections to the inferior colliculus following unilateral cochlear ablation in the neonatal gerbil *Meriones unguiculatus*. J Comp Neurol 214:144–153.

Pidoux B, Verley R, Farkas E, Scherrer J. 1979. Projections of the common fur of the muzzle upon the cortical area for mystacial vibrissae in rats dewhiskered since birth. Neurosci Lett 11:301–306.

Pidoux B, Diebler MF, Savy C, Farkas E, Verley R. 1980. Cortical organization of the postero-medial barrel-subfield in mice and its reorganization after destruction of vibrissal follicles after birth. Neuropathol Appl Neurobiol 6:93–107.

Rajan R, Irvine DRF, Wise LZ, Heil P. 1993. Effect of unilateral partial cochlear lesions in adult cats on the representation of lesioned and

unlesioned cochleas in primary auditory cortex. J Comp Neurol 338: 17–49.

Rasmusson D, Nance DM. 1986. Non-overlapping thalamocortical projections for separate forepaw digits before and after cortical reorganization in the raccoon. Brain Res Bull 16:399–406.

Robertson D, Irvine DRF. 1989. Plasticity of frequency organization in auditory cortex of guinea pigs with partial unilateral deafness. J Comp Neurol 282:456–471.

Schwaber MK, Garraghty PE, Kaas JH. 1993. Neuroplasticity of the adult primate auditory cortex following cochlear hearing loss. Am J Otol 14:252–258.

Shatz CJ, Stryker MP. 1978. Ocular dominance in layer IV of the cats visual cortex and the effects of monocular deprivation. J Physiol (Lond) 281:267–283.

Shook BL, Chalupa LM. 1986. Organization of geniculocortical connections following prenatal interruption of binocular interactions. Brain Res Dev Brain Res 28:47–62.

Stryker MP, Harris WA. 1986. Binocular impulse blockade prevents the formation of ocular dominance columns in cat visual cortex. J Neurosci 6:2117–2133.

Swindale NV. 1981. Absence of ocular dominance patches in dark-reared cats. Nature 290:332–333.

Trevelyan AJ, Thompson ID. 1992. Altered topography of the geniculocortical projection of the golden hamster following neonatal monocular enucleation. Eur J Neurosci 4:1104–1111.

Trune DR. 1982. Influence of neonatal cochlear removal on the development of mouse cochlear nucleus. I. Number, size, and density of its neurons. J Comp Neurol 209:409–242.

Waite PME, Taylor PK. 1978. Removal of whiskers in young rats causes functional changes in cerebral cortex. Nature 274:600–602.

Wiesel TN, Hubel DH. 1963a. Single-cell responses in striate cortex of kittens deprived of vision in one eye. J Neurophysiol 26:1003–1017.

Wiesel TN, Hubel DH. 1963b. Effects of visual deprivation on morphology and physiology of cells in the cats lateral geniculate body. J Neurophysiol 26:978–993.

Willott JF. 1984. Changes in frequency representation in the auditory system of mice with age-related hearing impairment. Brain Res 309: 159–162.

Winer, JA. 1985. The medial geniculate body of the cat. Adv Anat Embryol Cell Biol 86:1–98.

Winer JA, Sally SL, Larue DT, Kelly JB. 1999. Origins of medial geniculate body projections to physiologically defined zones of rat primary auditory cortex. Hearing Res 130:42–61.